Controlling the effective bending stiffness via out-of-plane rotational resonances in elastic metamaterial thin plates

Jinjie Shi, [1]Chenkai Liu,[1] and Yun Lai[2,1,*]

[1]College of Physics, Optoelectronics and Energy & Collaborative Innovation Center of Suzhou Nano Science and Technology, Soochow University, Suzhou 215006, Jiangsu, People's Republic of China

[2]National Laboratory of Solid State Microstructures, School of Physics, and Collaborative Innovation Center of Advanced Microstructures, Nanjing University, Nanjing 210093, Jiangsu, People's Republic of China

E-mail: laiyun@nju.edu.cn

Keywords: elastic metamaterial plate, bending stiffness

Abstract

In this work, we investigate the effective parameters of elastic metamaterial thin plates. We find that the out-of-plane rotational resonances can lead to a resonant behavior in the effective bending stiffness of metamaterial thin plates, which provides a route to tune the effective bending stiffness independently, from positive to negative values, and even infinity. By using resonant frequency analysis for metamaterial plates with different sizes, we have verified the resonant nature of the effective bending stiffness. Moreover, by designing a new type of elastic metamaterial plate with enhanced moment of inertia, we demonstrate a convenient way to tune the frequency regime of negative bending stiffness to overlap with that of negative mass density, and thus realize a band of negative group velocity. With the effective mass density and bending stiffness being independently tunable, the resonance properties of the elastic metamaterial thin plate can be engineered efficiently. Our work demonstrates a unique approach for manipulating flexural waves in elastic metamaterial thin plates.

Introduction

In the past few decades, metamaterials have been extensively investigated due to their unprecedented capability to control the propagation of electromagnetic, acoustic, and elastic waves. Metamaterials homogenized as effective media can exhibit exotic effective material parameters far beyond natural materials. For acoustic and elastic metamaterials, exotic parameters have been widely investigated, such as negative mass density [1-5], negative bulk modulus [6-8], negative shear modulus [9], extreme anisotropy [10-13], hybrid properties [14-16], etc. These unprecedented properties give rise to novel phenomena and applications such as low-frequency blocking [17,18], negative refraction [19-21], cloaking [22-28], perfect absorption [29-34], acoustic impedance matching effect [35], mode conversion [9,36] and topological effects [38-40], etc. The development in acoustic and elastic metamaterials significantly enriches the physics and may have important implications in acoustics, structural mechanics, architecture, seismology and other disciplines in the future.

Interestingly, in special geometric bodies composed of elastic metamaterials, such as metamaterial beams or metamaterial plates, some new phenomena absent in the bulk elastic

metamaterials may appear. For instance, in a recent experimental study on a beam structure composed of elastic metamaterials [15], besides the unusual transmission behaviors such as forbidden transverse or longitudinal waves, which also exist in bulk media [14], a unique vibrational property denoted as the torsional band gap was also observed, which is a unique phenomenon in the beam geometry. For flexural waves in elastic thin plates, the most important parameter besides the mass density per area $\bar{m}$ is the bending stiffness D (also denoted as flexural rigidity). The wave equation of the flexural waves in elastic thin plates is

$$\nabla^4 w + \frac{\bar{m}}{D}\frac{\partial^2 w}{\partial t^2} = 0 . \qquad (1)$$

Here, w is the deflection of the thin plate. For a homogeneous elastic thin plate, the bending stiffness can be obtained as $D = \frac{Eh^3}{12\left(1-\nu^2\right)}$, in which E is the Young's modulus, ν is the Poisson's ratio of the material and h is the thickness of the thin plate. Therefore, in previous researches on elastic metamaterial thin plates, the tunability of the bending stiffness is usually controlled by changing the Young's modulus [22,41-46]. However, since in the beam configuration, the bending stiffness is defined as $D = EI$, where I is the second moment of area of the beam's cross-section, which is related to the moment of inertia. This indicates that engineering the moment of inertia of metamaterial may give another approach for efficiently controlling the effective bending stiffness of the thin plate.

In this work, we investigate the effective parameters of elastic metamaterial thin plates. The elastic metamaterial thin plate with its unit cell structure is showed in Fig.1. Such a membrane-mass structure is known for exhibiting negative effective mass density due to dipolar resonances [5]. Interestingly, we show that the effective bending stiffness of the thin plate can be controlled independently and efficiently, by tuning the out-of-plane rotational resonance instead of the dipolar resonance, because such rotational resonances can lead to resonant behaviors in the effective moment of inertia. In order to prove this argument, we have performed resonant frequency analysis for elastic metamaterial thin plates with different sizes. Indeed, we observe a resonant behavior in the effective bending stiffness, which can vary from positive to negative values and even approach infinity. The resonant frequencies can thus be efficiently predicted and controlled by the effective parameters. In a second example, we have replaced the central steel plate with platinum cylinders with a suitable length. As a result, the out-of-plane rotational resonance is significantly enhanced and the frequency regime of negative bending stiffness is shifted lower to overlap with the regime of negative mass density. A negative band is realized due to double negativity. Our work demonstrates an efficient and systematic method to control the effective bending stiffness via out-of-plane rotational resonances instead of modulus. With the effective mass density and bending stiffness both being independently controllable, advanced manipulation of flexural waves in elastic thin plates is thus possible.

Results

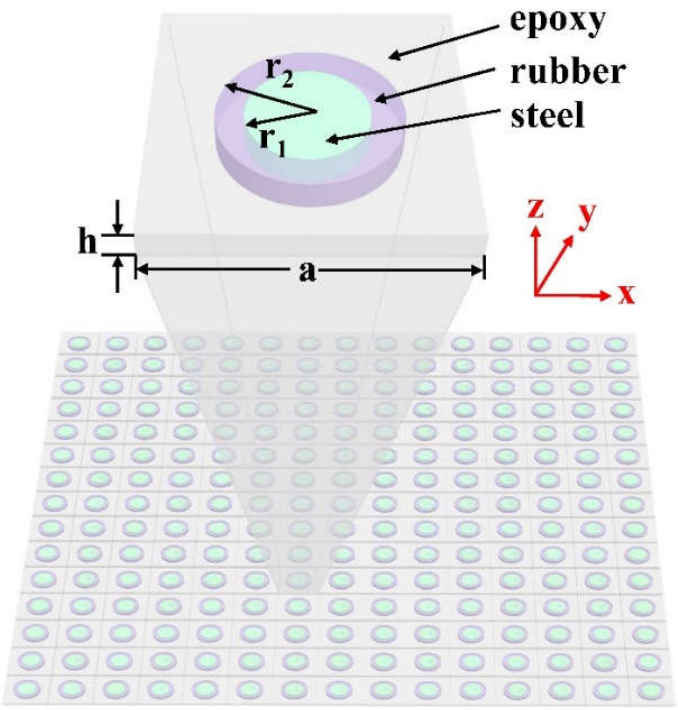

Fig. 1. Illustration of the elastic metamaterial thin plate and its unit cell.

Without loss of generality, we consider a membrane-mass-type thin plate, as shown in Fig.1. The plate is composed of a square lattice of metamaterial units. The unit cell is an epoxy thin plate embedded with a circular membrane of silicone rubber and a circular plate of steel which is placed at the center of the membrane. The lattice constant is set to be $a = 5\text{cm}$. The steel plate has a radius of $r_1 = 1\text{cm}$. The outer radius of the rubber membrane is $r_2 = 1.5\text{cm}$. The three components have the same thickness of h=0.5cm. The thin plate lies in the xy-plane with its normal direction defined as the z-axis. The material parameters are taken to be mass density ρ =7850 kg m^{-3}, the Young's modulus E = 180GPa, Poisson ratio ν = 0.25 for the steel; ρ =1245 kg m^{-3}, E=3.3Mpa, ν=0.477 for the silicone rubber; and ρ =1130 kg m^{-3}, E=3.8Gpa, ν=0.35 for the epoxy.

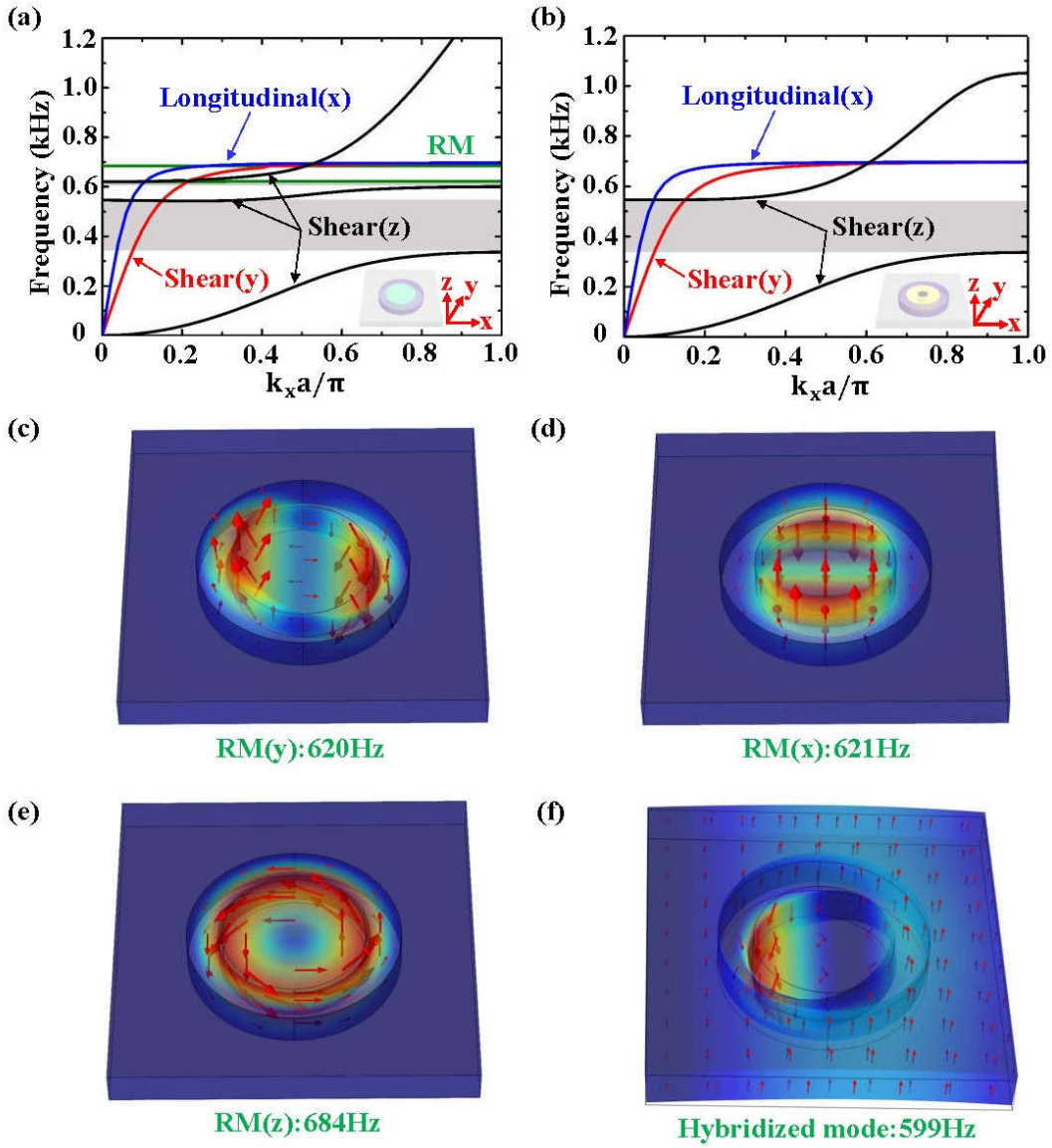

Fig. 2. The band structure and the field distributions of the metamaterial thin plate for some specific eigenstates. (a) The band structure of the elastic metamaterial thin plate. Black (Red) curves highlight the z-polarized (y-polarized) shear waves, respectively. Blue curve represents the longitudinal branch. Green curves show the resonant modes (RMs). The band gaps for z-polarized modes are marked in Grey. (b) The band structure of the metamaterial without the RMs. The proposed unit cell is showed in the lower right corner of Fig. 2(b). Here, two z-polarized shear bands are marked by black curves. Red/blue curve represents the y-polarized shear/longitudinal branch. The dark grey region are z-polarized shear bandgap. (c, d, e, f) The field distributions of the y-, x-, and z-polarized RMs (f=620Hz, f=621Hz and f=684Hz) at the Γ point, and the eigenfield of the hybridized mode (f=599Hz) at $k_x a/\pi = 0.9$, which is composed of y-polarized out-of-plane RM and z-polarized shear mode, respectively. Here, arrows indicate displacements and color indicates amplitude (red for large and blue for small).

We first calculate the band structure for such a metamaterial thin plate with infinite size. In Fig. 2(a), the solid line dispersion curve is numerically calculated by finite element analysis with commercial software COMSOL Multiphysics. We observe the following phenomena from Fig. 2(a). Firstly, there are two bulk shear branches (red and black curves), the other one is a longitudinal branch (blue curve). The y-polarized shear and longitudinal branches have linear dispersions, but the z-polarized shear branch has a quadratic dispersion in the quasi-static limit, which is consistent with the elastic theory of thin plates. Secondly, there are two band gaps for the z-polarized shear branch. The larger gap (337Hz-546Hz) and the smaller gap (600Hz-620Hz) are both marked in dark grey. Thirdly, besides the shear and longitudinal branches, there exist three resonant modes (RMs) (green curves) in the band structure. As we shall demonstrate, the y- and x-polarized out-of-plane RMs are important in controlling the bending stiffness of the thin plate.

The field distributions of the RMs at the Γ point are plotted in Figs. 2(c)-(f), respectively. Here, the color represents the amplitudes of displacements (blue/red for small/big values) and the arrows show the displacement vectors directly. The eigenstates in Fig. 2(c) (f=620Hz), Fig. 2(d) (f=621Hz) and Fig. 2(e) (f=684Hz) correspond to RMs whose rotational axes are the y-axis, x-axis and z-axis, respectively. Fig. 2(f) (f=599Hz) represents hybridized mode at $k_x a/\pi = 0.9$, which is composed of y-polarized out-of-plane RM and z-polarized shear mode.

As we have pointed out in previous works [15], RMs can change the effective moment of inertia of the thin plate. Since the bending stiffness D is related to both modulus and moment of inertia, the RMs will also have an influence on the effective bending stiffness.

In order to find out the physical origin of the two band gaps in Fig. 2(a), we have calculated the band structure for an almost equivalent elastic metamaterial except that it is designed with no RMs. The removing of RMs is obtained by replacing the original steel plate in Fig. 1 and Fig. 2(a) with a core shell structure, which is shown in Fig. 2(b). Such a core-shell structure has exactly the same weight as the original steel plate, but the mass density distribution is mostly concentrated inside a very small central area (the central dark core with a radius of 0.2cm). The outer radius of the very light part (the yellow shell) is set to be the same as the original structure, i.e. 1cm. The relevant material parameters are set as mass density ρ=1.8*10^5 kg m^{-3}, Young's modulus E = 180GPa, Poisson ratio ν = 0.25 for the central dark core, and ρ =677 kg m^{-3}, E=180GPa, ν=0.25 for the yellow shell.

This design could greatly reduce the moment of inertia of this unit cell, while keeping the other physical parameters to be almost the same. The band structure of this structure is showed in Fig. 2(b). Obviously, the lower band gap is almost exactly the same as that in the original structure (337Hz-546Hz). However, the original higher band gap (600Hz-620Hz) disappears. This result clearly proves that the higher band gap in the original structure is related to the RMs, while the lower band gap in both structures is independent of the RMs. As we shall show later, the two band gaps correspond to regions of negative bending stiffness and negative mass density, respectively.

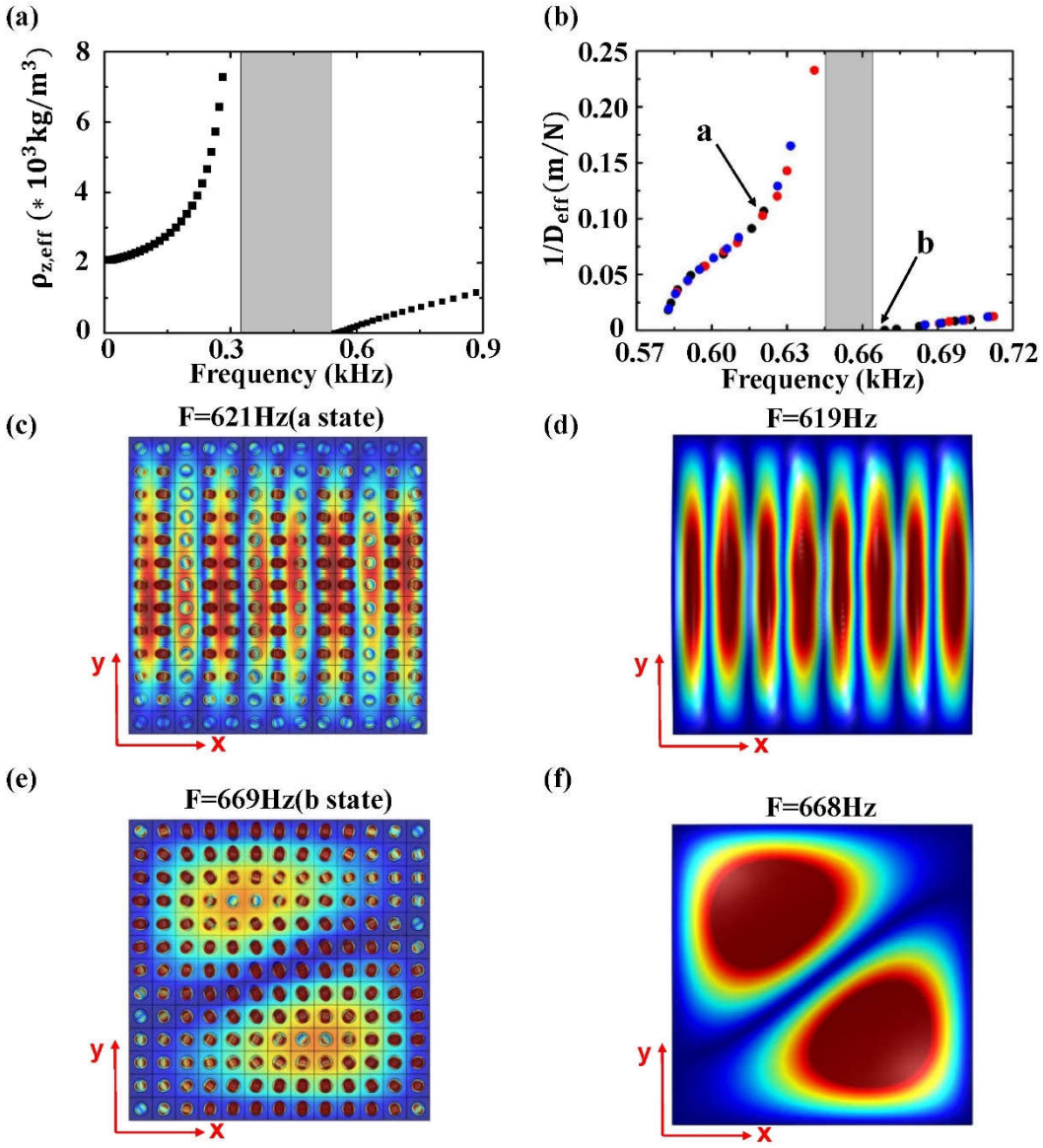

Fig. 3. (a) The obtained effective mass density in the z direction as a function of the frequency is described in Fig. 3(a). The dark grey region (337Hz-546Hz) represents the region with negative mass density. (b) The obtained effective bending stiffness from resonant frequency analysis. Black /red /blue dots represent the effective bending stiffness of plate with 13×13 / 15×15 / 18×18 unit cell, respectively. (c, e) The eigen-field distributions (f=621Hz and f=669Hz) of the elastic metamaterial thin plate (13×13 unit cell，b=0.65m). (d, f) The corresponding eigen-field distributions obtained with effective parameters (f=619Hz and f=668Hz).

The effective mass density can be obtained from the eigenmodes in the artificial structure without the RMs easily. Based on Newton's second law, the effective mass density satisfies,

$$\rho_{\mathrm{i}}^{\mathrm{eff}} = \frac{m_i^{eff}}{a^2 h} = \frac{F_i^{eff}}{\ddot{u}_i^{eff} a^2 h} = \frac{-F_i^{eff}}{\omega^2 u_i^{eff} a^2 h}, \quad \mathrm{i=x,\ y,\ z.} \qquad (2)$$

Here $\rho_{\mathrm{i}}^{\mathrm{eff}}$ and u_{i}^{eff} denote the effective mass density and the effective displacement of the

unit cell in the *i* direction, respectively. F_i^{eff} is the effective net force exerted on the unit cell in the *i* direction. Here, F_i^{eff} and u_i^{eff} can be obtained from the eigenmodes as,

$$F_i^{eff} = \int T_{ix} dydz\Big|_{x=a} - \int T_{ix} dydz\Big|_{x=0} \quad \text{and} \quad u_{\mathrm{i}}^{eff} = \frac{\int u_{\mathrm{i}} dydz\big|_{\mathrm{x=0}} + \int u_{\mathrm{i}} dydz\big|_{\mathrm{x=a}}}{2ah} \qquad (3)$$

for waves propagating in the x direction. Here, T_{ij} is the component of the stress tensor, with $i, j = x, y, z$. By applying Eqs. (2) and (3), the effective mass density in the z direction of the elastic metamaterial thin plate is plotted in Fig. 3(a). Here, we note that only the positive values of mass density are obtained because they are retrieved from the eigenmodes. However, since the mass density should obey the Lorentz model, obviously the mass density has a region of negative value between 337Hz and 546Hz (marked by dark grey region), which is consistent with the lower band gap. Therefore, the physical origin of the lower band gap lies in negative effective mass density of the thin plate.

In order to prove that the out-of-plane RMs will change the effective bending stiffness of the thin plate, we have conducted resonant frequency analysis for finite-sized samples with different sizes. Here, we consider the square elastic metamaterial thin plate is simply four-side-supported. And the boundary condition of the samples is:

$$(W)_{x=0} = 0; \qquad (4a)$$

$$(W)_{y=0} = 0, \qquad (4b)$$

where *W* denotes the displacement. We choose three thin plates with different sizes (13×13 / 15×15 / 18×18 unit cells) to investigate the resonant properties. We note that the bending stiffness, mass density, and resonant frequencies of a four-side-supported square thin plate are related by the following equation:

$$\omega_{mn} = \pi^2 \frac{m^2 + \mathrm{n}^2}{b^2} \sqrt{\frac{D_{\mathrm{eff}}}{\bar{m}}}. \qquad (5)$$

Here, ω_{mn} is the resonant frequency, *m* and *n* denote the order along the x and y directions, respectively. *b* is the side length of the thin plate. D_{eff} is the effective bending stiffness. And $\bar{m} = \rho_z^{eff} h$ is the mass density per unit area.

The resonant frequency ω_{mn} can be obtained by finite element analysis using Comsol Multiphysics. The order *m* and *n* can be determined from the eigen-field distributions. For examples, we show two eigen-field distributions at f=621Hz and 669Hz in Figs. 3(c) and 3(e). One can clearly count that *m=8* and *n=1* for the eigen-field of 621Hz; *m=1* and *n=2* for the eigen-field of 669Hz, respectively. Finally, by substituting the previously obtained effective mass density into Eq. (5), we can calculate the effective bending stiffness. The retrieved $1/D_{eff}$ is plotted in Fig. 3(b) for the three samples of 13×13(Black dots) / 15×15(red dots) /

18×18(blue dots) unit cells. Obviously, the $1/D_{eff}$ also obey the Lorentz model, and it has a negative value between 645Hz and 665Hz, in which there exists no resonant frequencies. It corresponds to the higher band gap in Fig. 2(a), although the frequency is shifted a little due to the finite-size effect or the simply supported boundary condition, which are nonexistent in infinite sample with periodic boundary conditions. From the region with resonant frequencies, we find that the obtained $1/D_{eff}$ is almost the same for the three samples of different sizes. The resonant behavior appears in $1/D_{eff}$ near the frequency of 620Hz, where the RMs exist. This indicates that the RM is indeed changing the effective bending stiffness significantly near its frequency. Such a change in bending stiffness will also significantly change the distribution of resonant modes. For instance, we choose two resonant frequencies (f=621Hz and f=669Hz), the eigen-field distributions are plotted in Figs. 3(c) and 3(e). At these two frequencies, the corresponding effective mass density and bending stiffness can be obtained in Figs. 3(a) and 3(b), as $\rho_z^{eff} = 284\ kg\ m^{-3}$ and $D_{eff} = 9.38\ N/m$; $\rho_z^{eff} = 470\ kg\ m^{-3}$ and $D_{eff} = 3042.7\ N/m$, respectively. The same eigen-field distribution can be obtained for a thin plate with $\rho = 284\ kg\ m^{-3}$ and $D = 9.32\ N/m$ at f=619Hz; $\rho = 470\ kg\ m^{-3}$ and $D = 3035\ N/m$ at 668Hz, respectively, as shown in Figs. 3(d) and 3(f). We note that due to the very small value of $1/D_{eff}$ at f=669Hz, the resonant mode has very small resonant order (*m=1* and *n=2*). While due to the large value of $1/D_{eff}$ at f=621Hz, the resonant mode has relatively large resonant order (*m=8* and *n=1*). Clearly, the effective bending stiffness can be tuned from positive (below band gap) to negative (band gap regime) and even to infinity (the upper band gap edge). And this resonant behavior in effective bending stiffness could dramatically change the resonant frequencies of the thin plate.

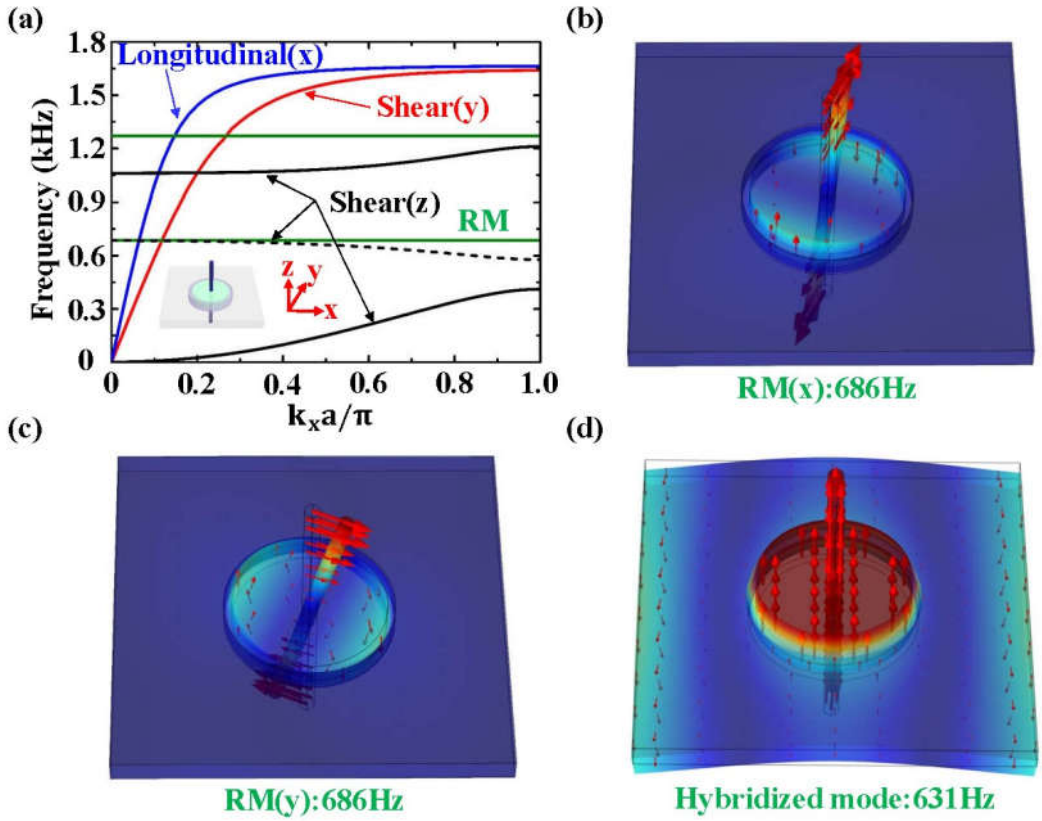

Fig. 4. The band structure of the metamaterial with a platinum cylinder at the centre and the field distributions of the metamaterial plate in some specific eigenstates. (a) The proposed unit cell is showed in the lower left corner of Fig. 4(a). Here, Black curves highlight the z-polarized shear waves. Black dashed line represents the negative band. Red/blue curve represents the y-polarized shear/longitudinal branch. The resonant modes (RMs) are marked by green curves. (b, c, d) The eigen-fields (f=686Hz, f=686Hz) at the Γ point in the two x- and y-polarized rotational bands and the hybridized mode eigen-field (f=631Hz) at $k_x a/\pi = 0.7$ in the negative band. Here, arrows represent displacements and color represents amplitude (blue for small and red for larger).

Discussion

In the above discussions, we have shown that the effective bending stiffness of elastic metamaterial thin plate can be controlled by out-of-plane RMs. In the following, we demonstrate an example on how to utilize this property to engineering the propagation of flexural waves in thin plates. Specifically, we find that the moment of inertia of the central mass plate can be enhanced significantly by extension in the z direction. The ratio between mass density and moment of inertia can be engineered in this approach. In the following, we have added a rod structure to the original central mass plate, as shown in the inset graph of Fig. 4(a). The moment of inertia is much enlarged when the rod is relatively long. In this way, the moment of inertia can be independently tuned with the mass density. In Fig. 4, we consider the case when a platinum rod is added at the center of the central mass plate. The material parameters are taken to be mass density ρ =2.145*10^4 kg m^{-3}, the Young's modulus E = 169GPa, Poisson ratio ν = 0.38 for the platinum. The radius of the platinum cylinder is

0.1cm and the height is 4cm. The outer radius of the steel (green part) is still 1cm, but the out radius of silicone rubber (purple part) reduces to 1.1cm. The lattice constant is 5cm and the plate thickness changes to 0.3cm. Fig. 4(a) shows the calculated band structure. Clearly, there is one negative band (black dashed line, 578Hz-685Hz) within the original first band gap induced by the negative mass density. This is because that the enhanced moment of inertia due to the platinum rod reduces the resonant frequency of the bending stiffness to be within the first band gap. At the same time, the reduced plate thickness and the outer radius of silicone rubber enlarges the bandwidth of the negative bending stiffness. As a result, a negative band appears due to double negativity in bending stiffness and mass density.

The eigen-fields can give a clear picture of the physical origin of the negative band. The field distributions of some specific eigen-fields at the Γ point and within the negative band are showed in Figs. 4(b)-6(d). Here, color indicates the amplitudes of displacements (blue/red for small/big values) and the arrows show the displacement vectors directly. The eigenstates (f=686Hz and f=686Hz, at the Γ point) in Figs. 4(b) and 4(c) are clearly rotational modes with x-axis and y-axis, respectively. The eigen-field (f=631Hz, at $k_x a/\pi = 0.7$) is a hybridized state of the y-polarized rotational mode and the z-polarized shear mode.

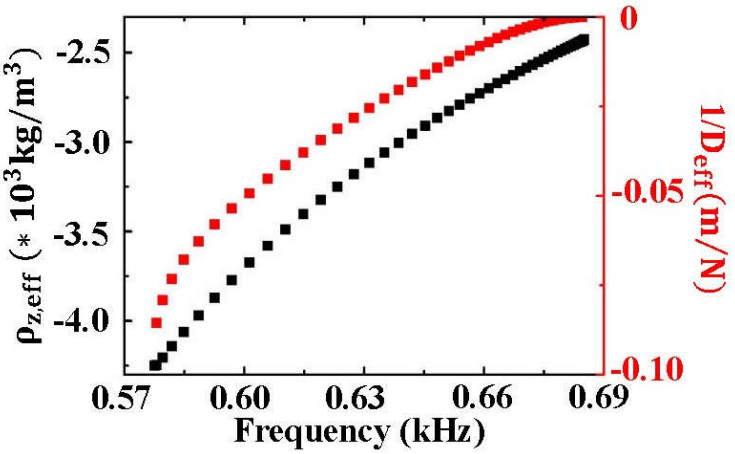

Fig. 5. For waves propagate in the x direction, the components of effective mass density in the z direction of the negative band (578Hz-685Hz) as function of frequency are described in Fig. 5 (black marks). The retrieved $1/D_{eff}$ within the negative band is also plotted in Fig. 5 (red marks).

In order to understand the physical origin of the negative band in Fig. 4(a) clearly, we have calculated the effective mass density in the z direction and bending stiffness. Here, the black marks represent the effective mass density in the z direction. Red marks are the retrieved $1/D_{eff}$ obtained by combining the mass density and the band structure in the dispersion relation of flexural waves $k^4 - \frac{\overline{m}}{D_{eff}}\omega^2 = 0$, which can be obtained from Eq. (1). We can clearly see that the effective mass density and bending stiffness are simultaneously negative within the negative band. The effective bending stiffness crosses zero at the upper

band edge. Obviously, the negative band is induced by double negativity in bending stiffness and mass density.

Conclusions

For conclusion, we have systematically investigated the resonant behaviors of an elastic metamaterial thin plate. Specifically, we prove that the effective bending stiffness of the metamaterial thin plate is closely related to the out-of-plane rotational resonances of the metamaterial. By engineering the out-of-plane rotational resonances, we can control the resonant behavior in the effective bending stiffness, independently with the effective mass density, which renders the resonant frequencies of the thin plate predictable and configurable. The effective bending stiffness can be tuned from positive to negative values, and even infinity. Realization of double negativity in bending stiffness and mass density has been shown to produce a negative band with negative group velocity. Our work demonstrates a novel design principle in controlling flexural waves in elastic thin plates, which could lead to important applications in acoustics and mechanical engineering.

Acknowledgements

This work is supported by National Key R&D Program of China (2017YFA0303702), National Natural Science Foundation of China (NSFC) (61671314, 11634005); Priority Academic Program Development of Jiangsu Higher Education Institutions (PAPD).

References

[1] Liu Z Y, Zhang X X, Mao Y W, Zhu Y Y, Yang Z Y, Chan C T and Sheng P 2000 *Science* **289** 1734-6

[2] Yang Z, Mei J, Yang M, Chan N H and Sheng P 2008 *Phys. Rev. Lett.* **101** 204301

[3] Lee S H, Park C M, Seo Y M, Wang Z G and Kim C K 2010 *Phys. Rev. Lett.* **104** 054301

[4] Liu X, Hu G K, Huang G L and Sun C T 2011 *Appl. Phys. Lett.* **98** 251907

[5] Yang M, Ma G C, Yang Z Y and Sheng P 2013 *Phys. Rev. Lett.* **110** 134301

[6] Fang N, Xi D J, Xu J Y, Ambati M, Srituravanich W, Sun C and Zhang X 2006 *Nat. Mater.* **5** 452-6

[7] Ding Y Q, Liu Z Y, Qiu C Y and Shi J 2007 *Phys. Rev. Lett.* **99** 093904

[8] Lee S H, Park C M, Seo Y M, Wang Z G and Kim C K 2009 *J. Phys.: Condens. Matter* **21** 175704

[9] Wu Y, Lai Y and Zhang Z Q 2011 *Phys. Rev. Lett.* **107** 105506

[10] Li J S, Fok L, Yin X B, Bartal G and Zhang X 2009 *Nat. Mater.* **8** 931-4

[11] Christensen J and de Abajo E J G 2012 *Phys. Rev. Lett.* **108** 124301

[12] Garcia-Chocano V M, Christensen J and Sanchez-Dehesa J 2014 *Phys. Rev. Lett.* **112** 144301

[13] Shen C, Xie Y B, Sui N, Wang W Q, Cummer S A and Jing Y 2015 *Phys. Rev. Lett.* **115** 254301

[14] Lai Y, Wu Y, Sheng P and Zhang Z Q 2011 *Nat. Mater.* **10** 620-4

[15] Ma G C, Fu C X, Wang G H, del Hougne P, Christensen J, Lai Y and Sheng P 2016 *Nat. Commun.* **7** 13536

[16] Ma G C, Yang M, Xiao S W, Yang Z Y and Sheng P 2014 *Nat. Mater.* **13** 873-8

[17] Cheng Y, Zhou C, Yuan B G, Wu D J, Wei Q and Liu X J 2015 *Nat. Mater.* **14** 1013
[18] Liu C K, Bai P and Lai Y 2016 *EPL (Europhysics Letters)* **115** 58002
[19] Zhang S, Yin L L and Fang N 2009 *Phys. Rev. Lett.* **102** 194301
[20] Zhu R, Liu X N, Hu G K, Sun C T and Huang G L 2014 *Nat. Commun.* **5** 5510
[21] Kaina N, Lemoult F, Fink M and Lerosey G 2015 *Nature* **525** 77
[22] Farhat M, Guenneau S and Enoch S 2009 *Phys. Rev. Lett.* **103** 024301
[23] Farhat M, Guenneau S, Enoch S and Movchan A B 2009 *Phys. Rev. B.* **79** 033102
[24] Cummer S A and Schurig D 2007 *New J. Phys.* **9** 45
[25] Zhang S, Xia C G and Fang N 2011 *Phys. Rev. Lett.* **106** 024301
[26] Zigoneanu L, Popa B I and Cummer S A 2014 *Nat. Mater.* **13** 352-5
[27] Jiang X, Liang B, Zou X Y, Yin L L and Cheng J C 2014 *Appl. Phys. Lett.* **104** 083510
[28] Shen C, Xu J, Fang N X and Jing Y 2014 *Phys. Rev. X* **4** 041033
[29] Mei J, Ma G C, Yang M, Yang Z Y, Wen W J and Sheng P 2012 *Nat. Commun.* **3** 756
[30] Song J Z, Bai P, Hang Z H and Lai Y 2014 *New J. Phys.* **16** 033026
[31] Wei P J, Croenne C, Chu S T and Li J S 2014 *Appl. Phys. Lett.* **104** 121902
[32] Duan Y T, Luo J, Wang G H, Hang Z H, Hou B, Li J S, Sheng P and Lai Y 2015 *Sci. Rep.* **5** 12139
[33] Yang M, Meng C, Fu C X, Li Y, Yang Z Y and Sheng P 2015 *Appl. Phys. Lett.* **107** 104104
[34] Leroy V, Strybulevych A, Lanoy M, Lemoult F, Tourin A and Page J H 2015 *Phys. Rev. B* **91** 020301
[35] Bok E, Park J J, Choi H, Han C K, Wright O B and Lee S H 2018 *Phys. Rev. Lett.* **120** 044302
[36] Kweun J M, Lee H J, Oh J H, Seung H M and Kim Y Y 2017 *Phys. Rev. Lett.* **118** 205901
[37] Lu J Y, Qiu C Y, Ye L P, Fan X Y, Ke M Z, Zhang F and Liu Z Y 2016 *Nat. Phys.* **13** 369-74
[38] Deng Y C, Ge H, Tian Y, Lu M H and Jing Y 2017 *Phys. Rev. B.* **96** 184305
[39] Li F, Huang X Q, Lu J Y, Ma J H and Liu Z Y 2017 *Nat. Phys.* **14** 30
[40] Lu J Y, Qiu C Y, Deng W Y, Huang X Q, Li F, Zhang F, Chen S Q and Liu Z Y 2018 *Phys. Rev. Lett.* **120** 116802
[41] Qian W, Yu Z Y, Wang X Y, Lai Y and Yellen B B 2016 *J. Appl. Phys.* **119** 1734
[42] Chen Y Y, Hu G K and Huang G L 2017 *J. Mech. Phys. Solids* **105** 179-98
[43] Wang Z W, Zhang Q, Zhang K and Hu G K 2016 *Adv. Mater.* **28** 9857
[44] Li X P, Chen Y Y, Hu G K and Huang G L 2018 *Smart Mater. Struct.* **27** 055010
[45] Zhu R, Chen Y Y, Barnhart M V, Hu G K, Sun C T and Huang G L 2016 *Appl. Phys. Lett.* **108** 011905
[46] Chen Y Y, Zhu R, Barnhart M V and Huang G L 2016 *Sci. Rep.* **6** 35048